Electronic Supplementary Information

for

Rational Design of Lanthanide-Based Metal Organic Frameworks for CO_2 Capture Using Computational Modeling

Zeynep Pinar Haslak,† Hasan Can Gulbalkan,† and Seda Keskin*

Department of Chemical and Biological Engineering, Koc University, Rumelifeneri Yolu, Sariyer, 34450, Istanbul, Turkey

†These authors contributed equally.

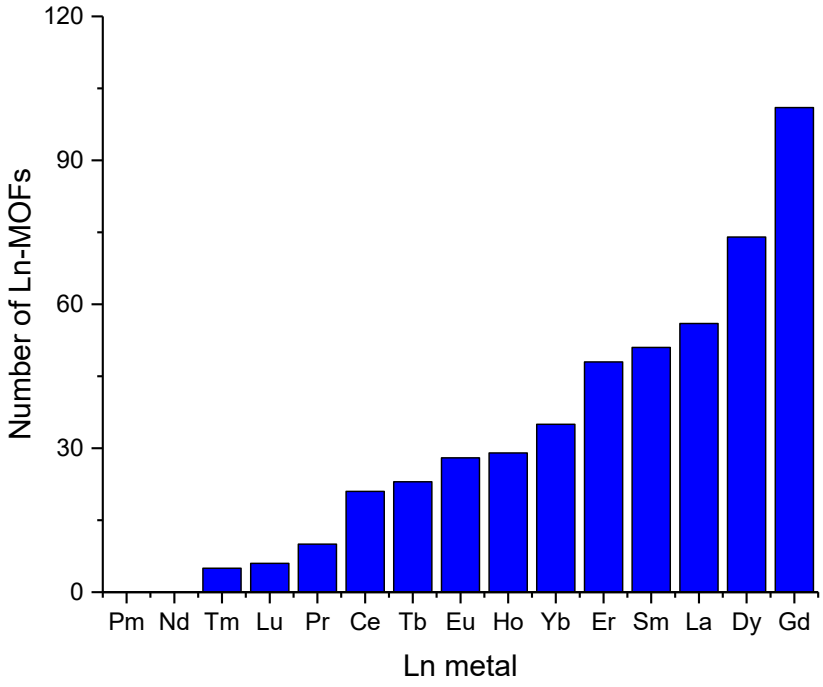

Figure S1. Distribution of lanthanide metals in 487 MOFs.

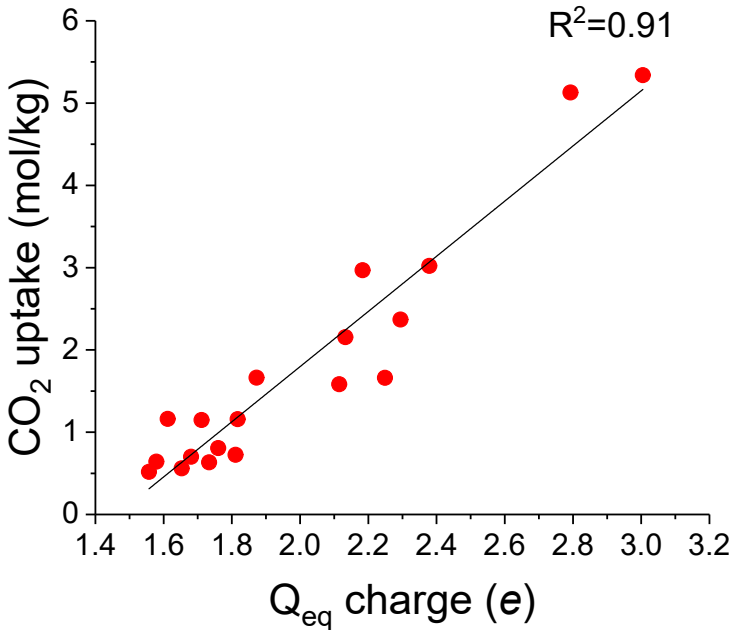

Figure S2. Relationship between Q_{eq} charge on lanthanide metal and CO_2 uptake at 1 bar.

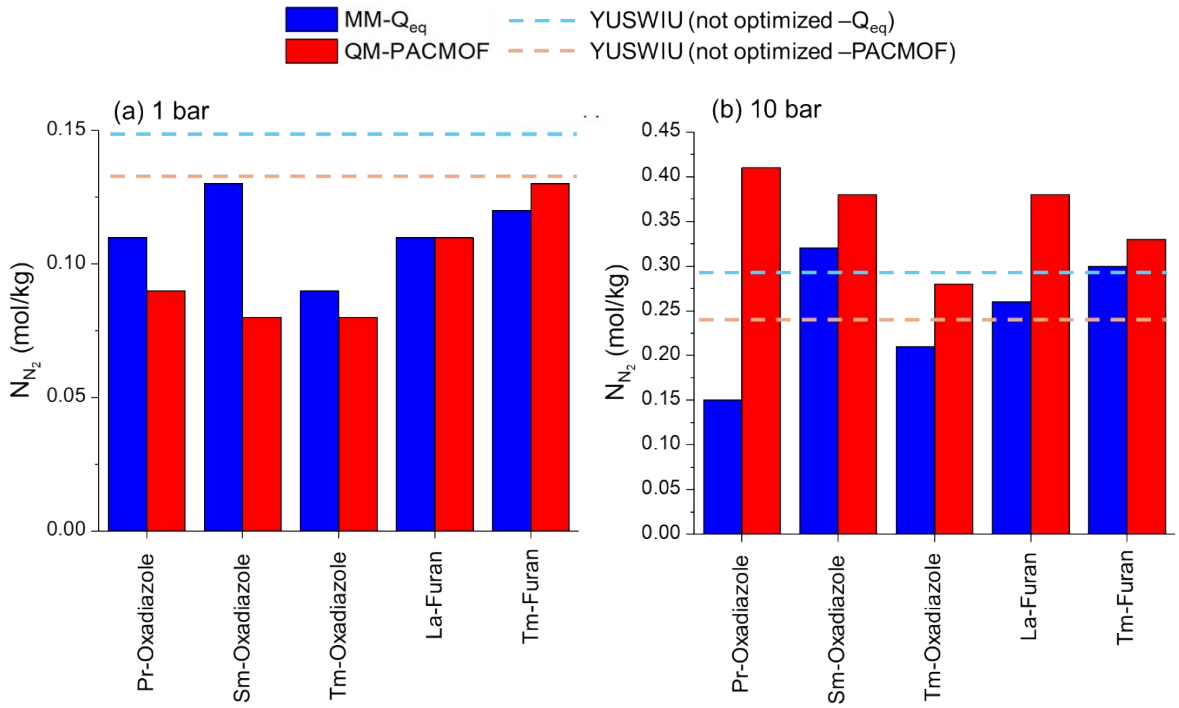

Figure S3. Calculated N_2 uptakes at (a) 1 bar, (b) 10 bar for original YUSWIU and YUSWIU-derived hypothetical MOFs.

Table S1. Gas separation performance metrics computed to evaluate Ln-MOFs.

Metric	Formula
Mixture adsorption selectivity	$S_{ads,CO_2/N_2}^{mix} = \frac{N_{CO_2}}{N_{N_2}} / \frac{y_{CO_2}}{y_{N_2}}$
Working capacity	$\Delta N_{CO_2} = N_{ads,CO_2} - N_{des,CO_2}$
Adsorbent performance score	$APS = S_{ads,CO_2/N_2}^{mix} \times \Delta N_{CO_2}$
Percent regenerability	$R\% = \frac{\Delta N_{CO_2}}{N_{ads,CO_2}} \times 100\%$

$N_{ads,i}$: gas uptake at adsorption condition (mol/kg), $N_{des,i}$: gas uptake at desorption condition (mol/kg), y: bulk composition of the gas mixture.

Table S2. Calculated adsorbent performance metrics and structural properties of top 25 Ln-MOFs for CO_2/N_2 separation at VSA condition.

MOFs	APS (mol/kg)	$S_{ads, CO_2/N_2}$	ΔN_{CO_2} (mol/kg)	R (%)	LCD (Å)	PLD (Å)	S_{acc} (m^2/g)	ϕ
Vacuum swing adsorption (VSA)								
WASTUG	843	324	2.60	83	10.47	7.26	1221	0.67
LIBQIY	794	217	3.66	76	9.48	4.10	1668	0.70
NAQQED	732	197	3.72	88	8.85	4.19	1706	0.70
FEDBEX	697	325	2.14	76	5.55	5.04	805	0.56
VEHRIL	529	170	3.11	81	8.80	4.02	1718	0.69
SEHSOO	522	140	3.73	84	5.47	4.62	1383	0.63
NAQRAA	385	134	2.87	89	8.82	4.19	1851	0.70
SEHSUU	371	113	3.29	86	5.45	4.60	1367	0.63
SOZGOF	268	82	3.28	78	8.62	3.76	1430	0.63
VUGWUR	254	73	3.47	80	7.84	6.35	1068	0.57
COWMIL	251	106	2.38	75	6.74	5.53	1542	0.65
SOXDEQ	234	120	1.95	80	7.83	4.20	484	0.46
ABEYIR	230	170	1.35	85	4.70	3.92	272	0.47
KULRIT	229	91	2.51	84	5.78	3.79	983	0.59
SOTXAC	217	99	2.20	78	6.13	5.14	1490	0.65
COWMOR	200	91	2.21	80	6.72	5.56	1534	0.65
TAZLUD	188	82	2.28	83	11.12	6.79	2132	0.73
FOXNIQ	169	178	0.95	79	5.68	4.35	230	0.44
LADQIT	168	76	2.22	82	6.45	5.56	533	0.57
DALVIY	158	80	1.98	77	8.33	5.09	1829	0.66
DODMIT	156	88	1.77	75	7.01	4.52	719	0.54
OJONOQ	155	136	1.14	89	6.44	5.38	1006	0.67
YUSWIU	146	80	1.83	85	5.64	4.78	940	0.56
QUZVEO	146	98	1.49	78	9.49	8.84	1015	0.61
NUCYER	145	135	1.08	77	4.97	4.20	323	0.49

Table S3. Selected bond lengths (Å) for MM-level optimized geometries of Ln-YUSWIU.

Ln	Ln—O Largest	Ln—O Shortest	Ln—Ln
La	2.343	2.429	4.606
Ce	2.275	2.359	4.516
Pr	2.268	2.355	4.501
Sm	2.253	2.342	4.445
Eu	2.312	2.407	4.508
Gd	2.284	2.368	4.333
Tb	2.245	2.332	4.370
Dy	2.388	2.220	4.317
Ho	2.245	2.328	4.303
Er	2.246	2.328	4.288
Tm	2.251	2.343	4.280
Yb	2.652	2.711	4.946
Lu	2.061	2.141	2.701

Table S4. Selected bond lengths (Å) for MM-level optimized geometries of generated Dy-MOFs.

Dy-MOF	Dy—O Largest	Dy—O Shortest	Dy—Dy
Dy-Aminetriazole	2.405	2.259	4.522
Dy-Oxadiazole	2.318	2.222	4.438
Dy-Methyltriazole	2.347	2.253	4.412
Dy-Furan (YUSWIU)	2.388	2.220	4.317
Dy-Pyrrole	2.342	2.242	4.222
Dy-Isoindoline	2.343	2.286	4.038

Table S5. Calculated adsorbent performance metrics and structural properties of generated 37 Ln-MOFs for CO_2/N_2 separation at VSA condition. Geometries are optimized at MM-level.

Ln-MOFs	APS (mol/kg)	$S_{ads,CO_2/N_2}$	LCD (Å)	PLD (Å)	S_{acc} (m^2/g)	ϕ
Ce-Aminetriazole	38	47	5.04	4.44	511	0.51
Ce-Pyrrole	1023	595	5.83	5.24	1066	0.58
Dy-Aminetriazole	12	25	5.23	4.45	509	0.51
Dy-Oxadiazole	88	62	5.72	5.17	919	0.58
Dy-Pyrrole	15	23	5.78	5.15	932	0.57
Er-Aminetriazole	116	119	5.14	3.74	125	0.47
Er-Furan	13	21	5.89	5.11	1043	0.58
Er-Oxadiazole	40	39	5.70	5.13	901	0.58
Er-Pyrrole	9	18	5.78	5.14	912	0.57
Eu-Aminetriazole	25	38	5.24	4.53	559	0.52
Eu-Pyrrole	917	510	5.88	5.27	1032	0.58
Gd-Furan	11	19	5.94	5.17	1101	0.59
Gd-Oxadiazole	40	39	5.67	5.14	951	0.59
Gd-Pyrrole	8	16	5.81	5.18	960	0.58
Ho-Aminetriazole	25	39	5.58	5.02	468	0.52
Ho-Furan	17	24	5.89	5.12	1053	0.58
Ho-Oxadiazole	40	39	5.66	5.05	890	0.58
Ho-Pyrrole	11	20	5.77	5.13	912	0.57
La-Aminetriazole	31	42	4.87	4.63	491	0.51
La-Furan	427	197	6.12	5.33	1226	0.60
La-Pyrrole	435	184	6.06	5.22	1201	0.60
Lu-Aminetriazole	15	27	4.95	4.67	323	0.46
Lu-Furan	42	40	5.18	4.29	417	0.49
Lu-Pyrrole	42	40	5.16	4.27	431	0.49
Pr-Aminetriazole	71	68	5.03	4.41	504	0.51
Pr-Oxadiazole	334	149	5.69	4.87	873	0.56
Sm-Aminetriazole	16	29	5.22	4.41	517	0.51
Sm-Furan	140	76	5.96	5.18	1124	0.59
Sm-Oxadiazole	255	131	5.77	5.28	982	0.59
Sm-Pyrrole	74	53	5.81	5.20	998	0.58
Tb-Aminetriazole	31	43	5.30	4.44	505	0.51
Tm-Furan	236	117	5.94	5.06	1068	0.59
Tm-Oxadiazole	310	195	5.68	5.13	901	0.58
Tm-Pyrrole	92	62	5.79	5.14	912	0.57
Yb-Aminetriazole	66	71	5.78	4.52	316	0.52
Yb-Furan	25	33	6.41	5.74	1332	0.63
Yb-Oxadiazole	68	52	5.61	5.20	1074	0.60

Table S6. Calculated adsorbent performance metrics for CO_2/N_2 separation and structural properties of 5 Ln-MOFs common under VSA and PSA conditions. Geometries were optimized at MM-level* and Q_{eq} charges were assigned.

Ln-MOFs	APS (mol/kg) (VSA)	APS (mol/kg) (PSA)	$S_{ads,CO_2/N_2}$ (VSA)	$S_{ads,CO_2/N_2}$ (PSA)	LCD (Å)	PLD (Å)	S_{acc} (m^2/g)	ϕ
Pr-Oxadiazole	334	500	149	198	5.69	4.87	873	0.56
Sm-Oxadiazole	255	202	131	91	5.77	5.28	982	0.59
Tm-Oxadiazole	310	223	195	128	5.68	5.13	901	0.58
La-Furan	427	402	197	145	6.12	5.33	1226	0.60
Tm-Furan	236	224	117	93	5.94	5.06	1068	0.59
Dy-Furan (YUSWIU)	146	200	80	88	5.64	4.78	940	0.56

*Data provided for YUSWIU were taken from the calculations performed for the Q_{eq} assigned crystal structure.

Table S7. Calculated adsorbent performance metrics and structural properties of promising generated Ln-MOFs for CO_2/N_2 separation at VSA condition. Geometries were optimized at QM-level* and PACMOF charges were assigned.

Ln-MOFs	APS (mol/kg) (VSA)	APS (mol/kg) (PSA)	$S_{ads,CO_2/N_2}$ (VSA)	$S_{ads,CO_2/N_2}$ (PSA)	LCD (Å)	PLD (Å)	S_{acc} (m^2/g)	ϕ
Pr-Oxadiazole	307	231	175	79	6.58	5.84	1382	0.64
Sm-Oxadiazole	296	195	200	80	6.31	5.68	1273	0.63
Tm-Oxadiazole	409	284	188	108	6.27	5.50	1166	0.62
La-Furan	334	339	161	99	6.06	5.21	1438	0.62
Tm-Furan	115	298	77	88	5.82	5.01	1118	0.60
Dy-Furan (YUSWIU)	248	208	116	106	5.64	4.78	940	0.56

*Data provided for YUSWIU were taken from the calculations performed for the PACMOF assigned crystal structure.

Table S8. Comparison between the highest positive and the lowest negative charges along with K_{CO_2} and K_{N_2} values for the five promising structures.

Ln-MOFs	K_{CO_2} (mol/kg/Pa)	K_{N_2} (mol/kg/Pa)	Highest positive charge	Lowest negative charge
La-Furan (QM-PACMOF)	7.0×10^{-4}	2.2×10^{-6}	La (+2.01)	O (-0.57)
La-Furan (QM-Q_{eq})	2.7×10^{-4}	2.1×10^{-6}	La (+1.72)	O (-0.63)
Tm-Furan (QM-PACMOF)	1.4×10^{-4}	2.0×10^{-6}	Tm (+2.10)	O (-0.70)
Tm-Furan (QM-Q_{eq})	6.2×10^{-5}	2.0×10^{-6}	Tm (+1.73)	O (-0.47)
Pr-Oxadiazole (QM-PACMOF)	8.2×10^{-4}	1.6×10^{-6}	Pr (+2.03)	O (-0.59)
Pr-Oxadiazole (QM-Q_{eq})	6.8×10^{-3}	1.8×10^{-6}	Pr (+2.20)	O (-0.52)
Sm-Oxadiazole (QM-PACMOF)	1.5×10^{-3}	1.6×10^{-6}	Sm (+2.14)	O (-0.60)
Sm-Oxadiazole (QM-Q_{eq})	8.8×10^{-5}	1.5×10^{-6}	Sm (+1.60)	O (-0.41)
Tm-Oxadiazole (QM-PACMOF)	3.3×10^{-4}	1.7×10^{-6}	Tm (+2.15)	O (-0.60)
Tm-Oxadiazole (QM-Q_{eq})	1.4×10^{-4}	1.6×10^{-6}	Tm (+1.80)	O (-0.46)
La-Furan (MM-PACMOF)	2.6×10^{-4}	2.9×10^{-6}	La (+2.13)	O (-0.63)
La-Furan (MM-Q_{eq})	2.2×10^{-3}	3.2×10^{-6}	La (+2.40)	O (-0.57)
Tm-Furan (MM-PACMOF)	1.6×10^{-4}	2.6×10^{-6}	Tm (+2.23)	O (-0.69)
Tm-Furan (MM-Q_{eq})	3.2×10^{-4}	2.7×10^{-6}	Tm (+2.29)	O (-0.60)
Pr-Oxadiazole (MM-PACMOF)	4.6×10^{-5}	2.1×10^{-6}	Pr (+2.28)	O (-0.68)
Pr-Oxadiazole (MM-Q_{eq})	4.0×10^{-4}	3.1×10^{-6}	Pr (+3.87)	O (-0.85)
Sm-Oxadiazole (MM-PACMOF)	4.7×10^{-4}	2.4×10^{-6}	Sm (+2.36)	O (-0.65)
Sm-Oxadiazole (MM-Q_{eq})	8.5×10^{-4}	3.0×10^{-6}	Sm (+2.18)	O (-0.56)
Tm-Oxadiazole (MM-PACMOF)	5.6×10^{-4}	2.2×10^{-6}	Tm (+2.30)	O (-0.67)
Tm-Oxadiazole (MM-Q_{eq})	1.3×10^{-3}	3.0×10^{-6}	Tm (+2.38)	O (-0.57)

Table S9. Calculated CO_2 and N_2 isosteric heat of adsorption (Q_{st}, *kJ/mol*) values of promising Ln-MOFs for CO_2/N_2 separation at 1 bar and 10 bar. Geometries were optimized at QM level* and PACMOF charges were assigned.

Ln-MOFs	$Q_{st}^{CO_2}$ **(1 bar)**	$Q_{st}^{N_2}$ **(1 bar)**	$Q_{st}^{CO_2}$ **(10 bar)**	$Q_{st}^{N_2}$ **(10 bar)**
Pr-Oxadiazole	32.75	13.32	31.90	15.94
Sm-Oxadiazole	32.35	13.66	30.68	16.15
Tm-Oxadiazole	36.27	14.14	34.57	17.01
La-Furan	32.68	14.47	33.66	17.82
Tm-Furan	32.64	14.61	33.01	17.07
Dy-Furan (YUSWIU)	36.00	16.86	35.03	17.99

*Data provided for YUSWIU were taken from the calculations performed for the PACMOF assigned crystal structure.